Size-Dependent Superparamagnetic Properties of Mn Spinel Ferrite Nanoparticles Synthesized from Reverse Micelles

Chao Liu and Z. John Zhang*

School of Chemistry & Biochemistry, Georgia Institute of Technology, Atlanta, Georgia 30332-0400

Received December 1, 2000. Revised Manuscript Received April 18, 2001

$MnFe_2O_4$ nanoparticles in a size range of 4−14 nm have been synthesized from water-in-toluene reverse micelles by using sodium dodecylbenzenesulfonate (NaDBS) as surfactant. The blocking temperature, saturation magnetization, and coercivity of the nanoparticles are clearly size-dependent. The blocking temperature increases from 20 to 250 K when the mean size of the nanoparticles increases from 4.4 to 13.5 nm. The coercivity at 20 K increases from 30 to 300 Oe with increasing nanoparticle size. The field-dependent magnetization hysteresis disappears above the blocking temperature. Due to high saturation field, the saturation magnetization of the nanoparticles has been obtained by the extrapolation of the magnetization vs $1/H$ plot to $1/H = 0$. The saturation magnetization decreases with decreasing nanoparticle size. The high saturation field and the size-dependent saturation magnetization suggest the existence of a magnetically inactive layer on $MnFe_2O_4$ nanoparticles. The linear fitting of the saturation magnetization vs $1/d$ plot gives the thickness of this inactive layer as 0.45 nm.

Introduction

The relationship between the size and the physical properties of nanoparticles inevitably is the issue that always attracts great interest in fundamental science and in technological applications.[1,2] Magnetic nanoparticles usually have a single domain magnetic structure.[3] They provide great opportunities to understand magnetic properties at the atomic level without the interference from complicated domain wall movement, especially for studying the size-dependent magnetic properties. Certainly, some fundamental issues such as quantum tunneling of magnetization could be elucidated by studying magnetic nanoparticles.[4] A fundamental understanding to the magnetic properties of nanoparticles also can have a profound impact on modern technologies. For instance, the unique superparamagnetic relaxation of magnetic nanoparticles is critically related to the thermal stability of magnetic media in high-density data storage devices.[5] Furthermore, magnetic nanoparticles have great potential for applications in modern medical science such as acting as drug carriers for site-specific drug delivery.[6]

The size-dependent magnetic properties of Mn spinel ferrite ($MnFe_2O_4$) nanoparticles have attracted considerable attention in recent years. This is largely due to the controversy surrounding the size-dependent Curie temperature shifting in $MnFe_2O_4$ nanoparticles.[7−12] It has been demonstrated that rapid nucleation and growth in coprecipitation for forming $MnFe_2O_4$ nanoparticles can result in a metastable cation distribution,[13] and different cation distributions will alter the magnetic properties of $MnFe_2O_4$ nanoparticles greatly.[14] The studies on $MnFe_2O_4$ nanoparticles prepared by coprecipitation illustrate the close relationship between the magnetic properties and the crystal chemistry of nanoparticles, especially for a complex metal oxide system such as Mn spinel ferrite.[15] Regarding the magnetic properties of a spinel ferrite system, several factors have to be considered such as the chemical composition, cation distribution, oxidation states, and nanoparticle size.

The magnetic properties of $MnFe_2O_4$ nanoparticles have been studied on the samples that were synthesized by the coprecipitation method.[7−9,14] Although the co-

* To whom correspondence should be addressed. E-mail: john.zhang@chemistry.gatech.edu.

(1) Alivisatos, A. P. *Science* **1996**, *271*, 933.
(2) Shi, J.; Gider, S.; Babcock, K.; Awschalom, D. D. *Science* **1996**, *271*, 937.
(3) Leslie-Pelecky, D. L.; Rieke, R. D. *Chem. Mater.* **1996**, *8*, 1770.
(4) Tejada, J.; Ziolo, R. F.; Zhang, X. X. *Chem. Mater.* **1996**, *8*, 1784.
(5) Sun, S.; Murray, C. B.; Weller, D.; Folks, L.; Moser, A. *Science* **2000**, *287*, 1989.
(6) Häfeli, U.; Schütt, W.; Teller, J.; Zborowski, M., Eds. *Scientific and Clinical Applications of Magnetic Carriers;* Plenum: New York, 1997.
(7) Tang, Z. X.; Sorensen, C. M.; Klabunde, K. J.; Hadjipanayis, G. C. *Phys. Rev. Lett.* **1991**, *67*, 3602.
(8) Tang, Z. X.; Chen, J. P.; Sorensen, C. M.; Klabunde, K. J.; Hadjipanayis, G. C. *Phys. Rev. Lett.* **1992**, *68*, 3114.
(9) Kulkarni, G. U.; Kannan, K. R.; Arunarkavalli, T.; Rao, C. N. R. *Phys. Rev. B* **1994**, *49*, 724.
(10) Van der Zaag, P. J.; Noordermeer, A.; Johnson, M. T.; Bongers, P. F. *Phys. Rev. Lett.* **1992**, *68*, 3112.
(11) Brabers, V. A. M. *Phys. Rev. Lett.* **1992**, *68*, 3113.
(12) Van der Zaag, p. J.; Brabers, V. A. M.; Johnson, M. T.; Noordermeer, A.; Bongers, P. E. *Phys. Rev. B* **1995**, *51*, 12009.
(13) Zhang, Z. J.; Wang, Z. L.; Chakoumakos, B. C.; Yin, J. S. *J. Am. Chem. Soc.* **1998**, *120*, 1800.
(14) Chen, J. P.; Sorensen, C. M.; Klabunde, K. J.; Hadjipanayis, G. C.; Devlin, E.; Kostikas, A. *Phys. Rev. B* **1996**, *54*, 9288.
(15) Van Groenou, A. B.; Bongers, P. F.; Stuyts, A. L. *Mater. Sci. Eng.* **1968/69**, *3*, 317.

10.1021/cm0009470 CCC: $20.00
Published on Web 06/01/2001

precipitation synthesis provides a quick and easy way to prepare $MnFe_2O_4$ magnetic nanoparticles, it usually produces nanoparticles with large size distribution and less defined crystal chemistry. Because of the rapid formation of nanoparticles, the cation distribution in such $MnFe_2O_4$ samples tends to be random and far from the equilibrium state.[13] Recently, we have been able to synthesize $MnFe_2O_4$ nanoparticles by using a water-in-toluene reverse micelle method.[16] Since the growth of nanoparticles is relatively slow in reverse micelle synthesis, the obtained $MnFe_2O_4$ nanoparticles usually have an equilibrated cation distribution and a narrower size distribution. Moreover, these nanoparticles possess little lattice strain and, therefore, avoid unpredictable changes in magnetic properties that commonly come with the strain in the crystal lattice. Combined X-ray diffraction and transmission electron microscopy studies have shown the high quality of these nanoparticles. Each $MnFe_2O_4$ nanoparticle is a single crystal, and the size distribution of these nanoparticles is under 15%.

The $MnFe_2O_4$ nanoparticles prepared from the reverse micelle method show typical superparamagnetic properties. Such interesting and important magnetic properties make $MnFe_2O_4$ nanoparticles strong candidates for advanced technological applications, including ferrofluid technology,[17] magnetocaloric refrigeration,[18] contrast enhancement in magnetic resonance imaging (MRI),[19] and magnetically guided site-specific drug delivery.[6] We herein report the systematic studies on the size dependence of the superparamagnetic properties of these $MnFe_2O_4$ spinel ferrite nanoparticles. The mean particle size varies from 4.4 to 13.5 nm. The blocking temperature, saturation magnetization, and coercivity of the nanoparticles are clearly size-dependent. The blocking temperature increases from 20 to 250 K with increasing nanoparticle size. The coercivity and saturation magnetization at 20 K increase from 30 to 300 Oe and from 35 to 73 emu/g, respectively. The superparamagnetic behaviors of these $MnFe_2O_4$ nanoparticles are consistent with the Stoner−Wohlfarth theory on single domain magnetic particles.

Experimental Section

Synthesis of Magnetic Nanoparticles. $MnFe_2O_4$ spinel ferrite nanoparticles were synthesized by using a water-in-toluene reverse micelle method with sodium dodecylbenzenesulfonate (NaDBS, $[CH_3(CH_2)_{11}(C_6H_4)SO_3]Na$) as surfactant. The details for the synthesis can be found elsewhere.[16] The size of the $MnFe_2O_4$ nanoparticles was controlled by adjusting the volume ratio of water to toluene.

Neutron Diffraction. Neutron diffraction data were collected using the HB4 powder diffractometer at the High-Flux Isotope Reactor (HFIR) of Oak Ridge National Laboratory. The $MnFe_2O_4$ sample was placed in a vanadium can for data collection at room temperature over the 2θ range of 11° to 135° in steps of 0.05°. The wavelength was precisely determined to be 1.4997(1) Å based on the refinements of the Si standard. The data were corrected for the variation in detector efficiencies, which were determined using a vanadium standard.

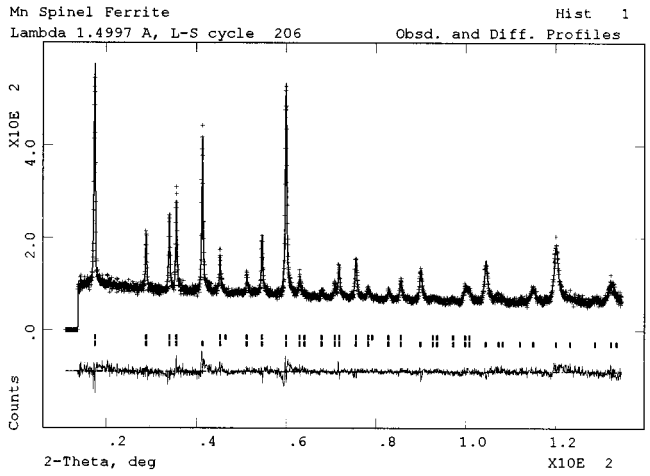

Figure 1. Neutron diffraction pattern of 13.5 nm $MnFe_2O_4$ nanoparticles at room temperature. The "goodness of fit", χ^2, is 1.35 and $R(f^2)$ is 0.0877. Below the pattern, the first row of sticks marks the peaks from the magnetic scattering of $MnFe_2O_4$ nanoparticles. And the second row of sticks corresponds to the peaks from the nuclear scattering.

Magnetic Measurement. Magnetic properties of the $MnFe_2O_4$ spinel ferrite nanoparticles were studied by using a Quantum Design MPMS-5S SQUID magnetometer with a magnetic field up to 5 T.

Results and Discussion

X-ray powder diffraction studies have confirmed that the $MnFe_2O_4$ nanoparticles synthesized from reverse micelles have the spinel structure. Elemental analysis by inductively coupled plasma−atomic emission spectroscopy (ICP−AES) has shown that the ratio of Mn to Fe is 1:2 in these $MnFe_2O_4$ nanoparticles. Mössbauer spectroscopy studies showed that all Fe cations were at their +3 oxidation state. The particle size was determined from peak broadening in X-ray powder diffraction pattern using the Scherrer equation. In addition to confirming the mean size of the $MnFe_2O_4$ nanoparticles, the bright field images from transmission electron microscopy (TEM) studies showed the size distribution to be less than 15%.

Neutron diffraction studies have been carried out to determine the magnetic structure and cation distribution in $MnFe_2O_4$ nanoparticles. Figure 1 displays the neutron diffraction pattern obtained at room temperature from the $MnFe_2O_4$ nanoparticles with a mean size of 13.5 nm. The Rietveld refinement shows that there is a well-defined magnetic order. The magnetic moment is 3.839 and $-3.217\ \mu_B$ at the tetrahedral and octahedral lattice site, respectively. The magnetic structure clearly indicates the antiferromagnetic exchange nature for the magnetic couplings between tetrahedral and octahedral lattice sites. The lattice constant for the cubic $MnFe_2O_4$ spinel unit cell is 8.4803(4) Å. As the size of the $MnFe_2O_4$ nanoparticles varies, the magnetic structure and cation distribution remain the same.

The temperature dependence of the magnetization of $MnFe_2O_4$ nanoparticles has been studied from 5 to 300−350 K. The nanoparticulate samples were initially cooled to 5 K without any magnetic field applied. After a magnetic field of 100 Oe was applied, the magnetization was recorded as the temperature slowly rises. The temperature-dependent magnetization is shown in Fig-

(16) Liu, C.; Zou, B.; Rondinone, A. J.; Zhang, Z. J. *J. Phys. Chem. B*, **2000**, *104*, 1141.
(17) Raj, K.; Moskowitz, R.; Casciari, R. *J. Magn. Magn. Mater.* **1995**, *149*, 174.
(18) McMichael, R. D.; Shull, R. D.; Swartzendruber, L. J.; Bennett, L. H. *J. Magn. Magn. Mater.* **1992**, *111*, 29.
(19) Mitchell, D. G. *J. Magn. Reson. Imaging* **1997**, *7*, 1.

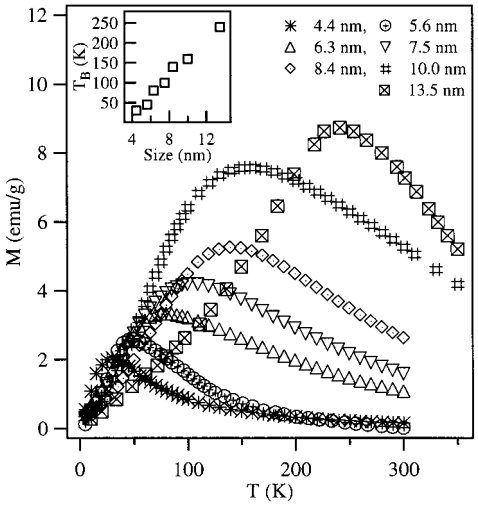

Figure 2. Magnetization vs temperature for $MnFe_2O_4$ nanoparticles with various sizes under a 100 G magnetic field. The inset shows the correlation between the blocking temperature and nanoparticle mean diameter.

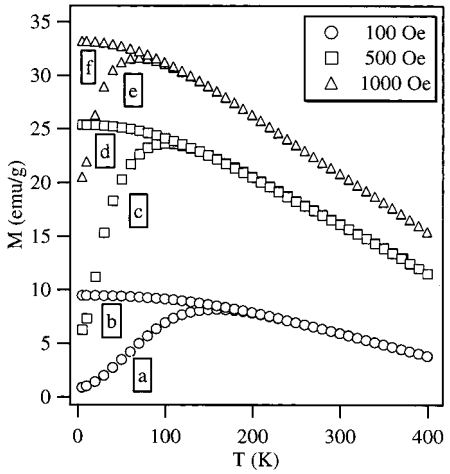

Figure 3. Temperature dependence of magnetization for zero-field-cooled (ZFC) and field-cooled (FC) 10 nm $MnFe_2O_4$ nanoparticles under various magnetic fields.

ure 2 for $MnFe_2O_4$ nanoparticles with various sizes. For all sizes of $MnFe_2O_4$ nanoparticles, the magnetization initially increases starting from 5 K. Eventually, the magnetization reaches the maximum point at certain temperature, which is defined as the blocking temperature, T_B. At the temperature above T_B, the $MnFe_2O_4$ nanoparticles show paramagnetic features. The blocking temperature increases with increasing mean size of the nanoparticle as the inset in Figure 2 displays.

The temperature-dependent magnetization of the $MnFe_2O_4$ nanoparticles clearly shows different behaviors under different cooling processes (Figure 3). For the measurements, the cooling of the nanoparticulate samples to the initial lowest measuring temperature can be with or without an applied magnetic field. After a zero-field-cooling (ZFC) process, the magnetization of the $MnFe_2O_4$ nanoparticles under a 100 Oe field increases with rising temperature. It reaches a maximum at the blocking temperature of these nanoparticles and then decreases (plot a in Figure 3). Plot b in Figure 3 shows the temperature-dependent magnetization behavior of the nanoparticles with a field-cooling (FC) process under a 100 Oe applied field. The magnetization

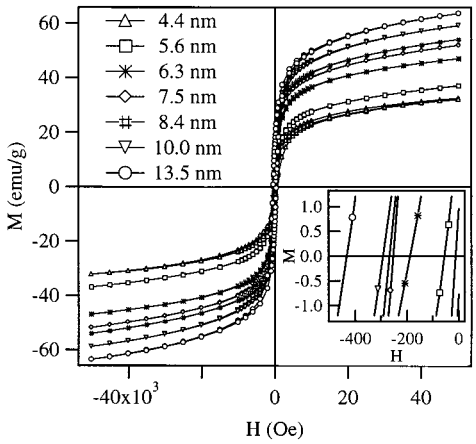

Figure 4. Field-dependent magnetization hysteresis of $MnFe_2O_4$ nanoparticles with various sizes at 20 K. The inset shows partial hysteresis curves at expanded scale of field strength.

under the same field maximizes at 5 K, and it decreases steadily with increasing temperature. After the temperature rises above the blocking temperature, the FC magnetization plot overlaps with the ZFC magnetization plot under the same magnetic field strength.

The blocking temperature of the $MnFe_2O_4$ nanoparticles depends on the strength of the applied magnetic field for the FC process and magnetization measurement. The blocking temperature is 170 K for $MnFe_2O_4$ nanoparticles with a mean size of 10 nm under an applied field of 100 Oe (plot a in Figure 3). The blocking temperature shifts down to 110 and 60 K when the applied field is increased to 500 and 1000 Oe, respectively (plot c and e in Figure 3). Large discrepancies are also clearly visible in temperature-dependent magnetization between ZFC and FC processes under a field of 500 and 1000 Oe.

$MnFe_2O_4$ nanoparticles show typical hysteresis for their field-dependent magnetization below the blocking temperature. Figure 4 shows the hysteresis loops of the $MnFe_2O_4$ nanoparticles with different mean sizes at 20 K under an applied magnetic field having a strength up to 5 T. The inset in Figure 4 displays the field dependence of magnetization of the $MnFe_2O_4$ nanoparticles plotted at a very small scale, which clearly shows that all these $MnFe_2O_4$ nanoparticles possess the coercivity at 20 K. As temperature increases, the coercivity steadily decreases. When temperature reaches the blocking temperature of the $MnFe_2O_4$ nanoparticles with a given mean size, the coercivity of these nanoparticles disappears. Figure 5 shows the field-dependent magnetization of $MnFe_2O_4$ nanoparticles with various mean sizes at 400 K. The coercivity has become zero, and the change of nanoparticle magnetization direction follows the orientation change of the applied magnetic field simultaneously.

The $MnFe_2O_4$ nanoparticles behave like an assembly of paramagnetic atoms at room temperature, which is higher above the blocking temperature for these $MnFe_2O_4$ nanoparticles at all sizes (Figure 2). However, the neutron diffraction studies clearly show a well-defined magnetic order in these nanoparticles at room temperature (Figure 1). These studies unambiguously show that the $MnFe_2O_4$ nanoparticles go through the superparamagnetic transition at the blocking temperature.[20]

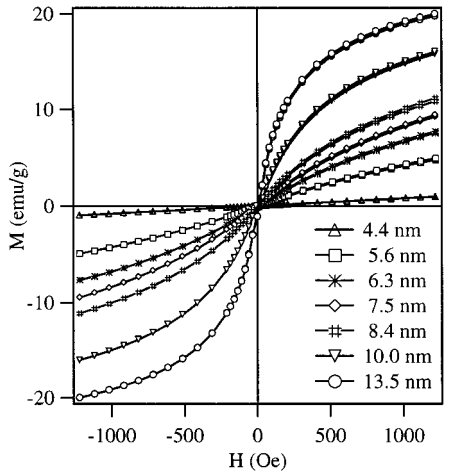

Figure 5. Field-dependent magnetization hysteresis of $MnFe_2O_4$ nanoparticles with various sizes at 400 K.

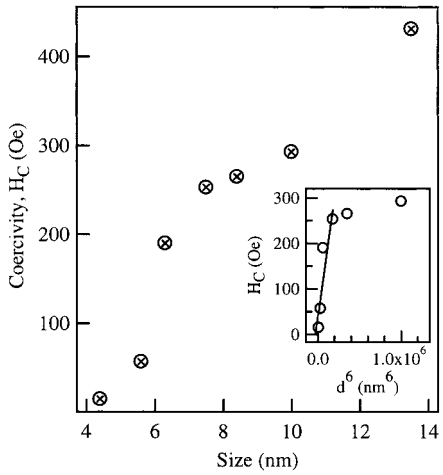

Figure 6. The correlation between the coercivity and the mean size of $MnFe_2O_4$ nanoparticles. The inset displays the plot of coercivity versus the sixth power of mean nanoparticle diameter.

The correlation between the blocking temperature and the size of the $MnFe_2O_4$ nanoparticles is consistent with the size dependence of the magnetocrystalline anisotropy in the nanoparticles (inset in Figure 2). According to the Stoner−Wohlfarth theory, the magnetocrystalline anisotropy (E_A) of a single domain particle can be expressed as

$$E_A = KV \sin^2 \theta \qquad (1)$$

where K is the magnetocrystalline anisotropy constant, V is the volume of the nanoparticle, and θ is the angle between the magnetization direction and the easy axis of the nanoparticle.[21] This anisotropy serves as the energy barrier to prevent the change of magnetization direction. When the size of the magnetic nanoparticles is reduced to a threshold value, E_A is comparable with the thermal activation energy, k_BT, with k_B being the Boltzman constant. Consequently, the magnetization direction of the nanoparticle can be easily moved away from the easy axis by thermal activation and/or by an external magnetic field.[22] The blocking temperature is the threshold point of thermal activation, at which magnetocrystalline anisotropy is overcome by thermal activation and the nanoparticles become superparamagnetic. The larger the nanoparticles are, the higher the E_A is. Consequently, a larger k_BT is required for superparamagnetic transition. Therefore, T_B increases with increasing nanoparticle size (inset in Figure 2).

The discrepant magnetization below the blocking temperature is a characteristic behavior of superparamagnetic nanoparticles having underwent different cooling processes. This discrepancy is due to the magnetic anisotropy energy barrier in $MnFe_2O_4$ nanoparticles.[22] The nanoparticles from a ZFC process need to overcome the magnetic anisotropy during the temperature-dependent magnetization measurement. The magnetic anisotropy does not have an effect on the magnetization of the nanoparticles from a FC process. Both thermal activation and applied magnetic field contribute to overcoming the magnetic anisotropy barrier in the zero-field-cooled nanoparticles. When a stronger magnetic field is applied, the magnetization direction of the nanoparticles becomes easier to switch to the field direction, and less assistance is required from thermal activation. Consequently, the blocking temperature shifts to a lower value with increasing strength of the applied field (Figure 3).

The hysteresis in the field-dependent magnetization of $MnFe_2O_4$ nanoparticles below the blocking temperature shows that the magnetic anisotropy prevents the magnetization direction of the nanoparticles to closely follow the direction of the applied magnetic field. The coercivity represents the certain strength of the field that is needed to surpass the anisotropy barrier and to allow the magnetization of the nanoparticles following the field orientation (Figure 4). Since the magnetic anisotropy is overcome above the blocking temperature, the hysteresis disappears and the direction of the nanoparticle magnetization changes simultaneously with the applied field (Figure 5).

The required field strength for switching the magnetization direction is surely higher at a given temperature as the magnetic anisotropy of the nanoparticles increases. Therefore, the coercivity of the $MnFe_2O_4$ nanoparticles increases with increasing nanoparticle sizes (Figure 6). For the nanoparticles with a mean size below 8 nm, the coercivity seems linearly dependent on the sixth power of the mean diameter of the $MnFe_2O_4$ nanoparticles (d^6) (Inset in Figure 6). Such a dependency may suggest that the exchange interaction between the nanoparticles has reduced the magnetic anisotropy of the small, randomly orientated $MnFe_2O_4$ nanoparticles.[23] However, further studies are certainly required before any firm conclusion can be drawn.

The saturation field of the $MnFe_2O_4$ nanoparticles can be obtained from a magnetization hysteresis measurement. Although $MnFe_2O_4$ in bulk form has the saturation field of about 0.5 T, the magnetization (M) measurements under a magnetic field (H) up to 5 T have not shown that the saturation magnetization was reached for the nanoparticles at various mean sizes

(20) Aharoni, A. *Introduction to the Theory of Ferromagnetism;* Oxford University Press: New York, 1996, p 92.
(21) Stoner, E. C.; Wohlfarth, E. P. *Philos. Trans. R. Soc. A*, **1948**, *240*, 599; reprinted in *IEEE Trans. Magn.* **1991**, *27*, 3475.
(22) Rondinone, A. J.; Samia, A. C. S.; Zhang, Z. J. *J. Phys. Chem. B* **1999**, *103*, 6876.
(23) Herzer, G. *J. Magn. Magn. Mater.* **1996**, *157/158*, 133.

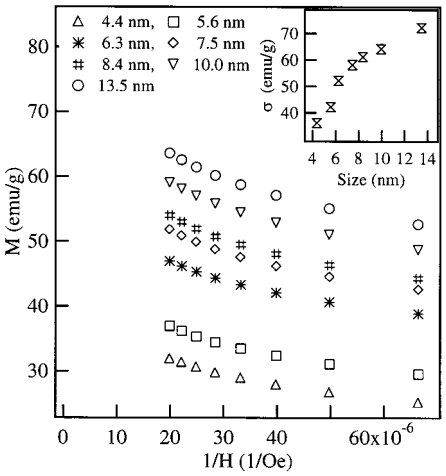

Figure 7. Plots of the magnetization of $MnFe_2O_4$ nanoparticles with various sizes at 20 K against the reciprocal of the applied magnetic field. The inset shows the correlation between the saturation magnetization and the mean nanoparticle size.

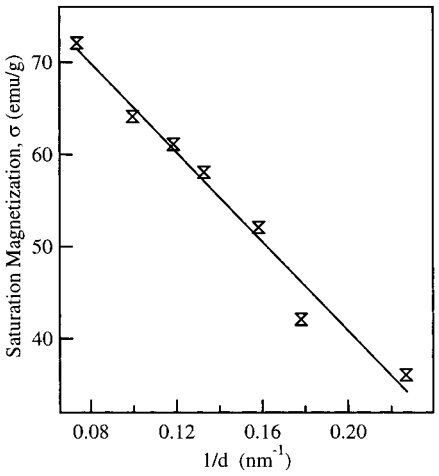

Figure 8. The linear correlation between the saturation magnetization and the reciprocal of the mean diameter of $MnFe_2O_4$ nanoparticles at 20 K.

(Figure 4). The unusually high saturation field in magnetic nanoparticles has been attributed to the existence of a magnetically inactive layer.[24] For $MnFe_2O_4$ nanoparticles, the saturation magnetization has been obtained through the extrapolation of the M vs $1/H$ plot to $1/H = 0$ (Figure 7). The saturation magnetization of $MnFe_2O_4$ nanoparticles decreases as the nanoparticles size decreases (inset in Figure 7). The size-dependent saturation magnetization has also been considered due to the $MnFe_2O_4$ nanoparticle having a magnetically inactive shell.[25] As the surface-to-volume ratio increases with decreasing nanoparticle size, the saturation magnetization decreases. The thickness (t) of this magnetically inactive layer can be derived from a linear fitting of the saturation magnetization plotted against $1/d$ (Figure 8).[14] The relationship between the saturation magnetization (σ_S) and the nanoparticle diameter (d) is

$$\sigma_S = \sigma_S(\text{bulk})(1 - 6t/d) \qquad (2)$$

From the data fitting, the derived bulk saturation magnetization, σ_S(bulk) is 89 emu/g at 20 K, which agrees with the literature reported values for bulk $MnFe_2O_4$ materials.[26] The thickness of the magnetically inactive layer is 0.45 nm. This number is comparable with the results obtained from a $MnFe_2O_4$ nanoparticle prepared by coprecipitation, which has an inactive layer of 0.5 nm at 10 K.[14] Certainly, the results from our field-dependent magnetization studies support the existence of a magnetically inactive layer on $MnFe_2O_4$ nanoparticles.

Conclusions

$MnFe_2O_4$ nanoparticles show typical size-dependent superparamagnetic properties. Their blocking temperature increases with increasing mean size of the nanoparticles. The coercivity decreases as temperature increases. Above the blocking temperature, the field-dependent magnetization hysteresis disappears and the coercivity becomes zero. The high saturation field and the size-dependent saturation magnetization suggest the existence of a magnetically inactive layer on $MnFe_2O_4$ nanoparticles. The linear fitting of the saturation magnetization vs $1/d$ plot gives the thickness of this inactive layer as 0.45 nm. The unambiguous superparamagnetic behavior certainly demonstrates $MnFe_2O_4$ nanoparticles as an excellent superparamagnetic nanoparticulate system for potential technological application such as MRI contrast enhancement and magnetically guided drug delivery.

Acknowledgment. We thank Dr. Bryan Chakoumakos of Oak Ridge National Laboratory for his help in neutron diffraction studies. We gratefully acknowledge the financial support in part from NSF (DMR-9875892) and the Beckman Young Investigator program of the Arnold and Mabel Beckman Foundation. TEM studies were carried out at the Electron Microscopy Center at Georgia Tech. Neutron diffraction studies were performed at Oak Ridge National Laboratory, which is managed by UT-Battelle, LLC for the U.S. Department of Energy under contract number DE-AC05-00OR22725.

CM0009470

(24) Kodama, R. H. *J. Magn. Magn. Mater.* **1999**, *200*, 359.
(25) Sato, T.; Iijima, T.; Seki, M.; Inagaki, N. *J. Magn. Magn. Mater.* **1987**, *65*, 252.
(26) Brabers, V. A. M. In *Handbook of Magnetic Materials*; Buschow, K. H. J., Ed.; North-Holland: Amsterdam, 1995; Vol. 8, p 213.